CHIN.PHYS.LETT. Vol. 25, No. 5 (2008) 1595

Detecting Determinism in Firing Activities of Retinal Ganglion Cells during Response to Complex Stimuli *

CAI Chao-Feng(蔡超峰), ZHANG Ying-Ying(张莹莹), LIU Xue(刘雪), LIANG Pei-Ji(梁培基), ZHANG Pu-Ming(张溥明)**

School of Life Science and Biotechnology, Shanghai Jiao Tong University, Shanghai 200240

(Received 23 January 2008)

Complex stimuli are used to probe the response properties of the chicken's retinal ganglion cells (GCs). The correlation dimension method and the nonlinear forecasting method are applied to detect the determinism in the firing activities of the retinal GCs during response to complex stimuli. The inter-spike interval (ISI) series and the first difference of the ISI (DISI) series are analysed. Two conclusions are drawn. Firstly, the first difference operation of the ISI series makes it comparatively easier for determinism detection in the firing activities of retinal GCs. Secondly, the nonlinear forecasting method is more efficient and reliable than the correlation dimension method for determinism detection.

PACS: 05. 45. −a, 05. 45. Tp

Traditionally, retinal ganglion cells (GCs) are studied using simple stimuli, such as spots or bars of light. However, retinal GCs are selectively driven by certain features (including size, direction and speed of motion, etc.) of the visual scene and thus studies using simple stimuli that do not contain the relevant features may not probe the response properties of the retinal GCs. A way that helps to resolve this problem is to use complex stimuli.[1] Complex stimuli refer to stimuli that contain rich structures in the stimuli domains, such as spatial position, orientation and frequency. The use of complex stimuli makes it possible to study the response properties of retinal GCs that cannot be probed by using simple stimuli.

As the final output neurons of the retina, GCs generate spikes to encode visual information. Thus, are there any deterministic components in the firing activities of retinal GCs? Answer to this question will be helpful to investigate the encoding mechanism of retinal GCs. With the development of nonlinear science, various methods have been developed and applied to detect the existence of determinism in a time series.[2−7] The most widely used method is the correlation dimension method proposed by Grassberger and Procaccia. They used correlation integrals to determine the attractor correlation dimension.[2] Another popular way is the nonlinear forecasting method originally developed by Sugihara and co-workers[3] and extended by Sauer.[4] Jeong and co-workers[5] developed a method based on the smoothness of the trajectory in phase space of a time series. Unfortunately, this method is not applicable to the inter-spike interval (ISI) series. Applying the correlation dimension method and the nonlinear forecasting method, researchers studied the ISI series derived from a single fiber of the injured sciatic nerves in the anesthetized rat.[6,7] Their results show that there exits determinism in the firing activities of sciatic nerves.

In this Letter, a multi-channel recording system is used to record the firing activities of chicken's retinal GCs during response to complex stimuli. The correlation dimension method and the nonlinear forecasting method are applied to analyse the ISI series derived from the recorded firing activities. The results show that neither the correlation dimension method nor the nonlinear forecasting method can provide any evidence for determinism in the ISI series. However, the nonlinear forecasting method demonstrates some weak but distinct determinism in the first difference of the ISI (DISI) series.

The detailed experimental procedure has been previously fully described.[8,9] In brief, extracellular recordings were made in isolated chicken retinas using a multi-electrode array (MEA, Multi Channel Systems MCS GmbH, Germany). The MEA consists of 60 electrodes (10 μm in diameter) arranged in an 8×8 matrix with 100 μm tip-to-tip distances. A small piece of retina quickly isolated from young born chicken (about 1–3 weeks) was attached with the GC side onto the surface of MEA. Two kinds of complex stimuli were used: (1) Grayscale natural movie (downloaded from website http://hlab.phys.rug.nl/vidlib/index.html, lasted for 192 s), (2) pseudorandom white-noise checker-board flickering (with 16×16 grid, lasted for 201 s). To characterize the underlying spatial and temporal features of the two kinds of stimuli, the normalized power spectral densities (PSDs) of each stimulus are calculated

*Supported by the National Basic Research Programme of China under Grant No 2005CB724301, the National Natural Science Foundation of China under Grant No 60775034.

**To whom correspondence should be addressed. Email: pmzhang@sjtu.edu.cn

and illustrated in Fig. 1. The stimuli are displayed on a computer monitor (796 FD Ⅱ, MAG) and then focused to form a 0.7×0.7 mm image onto the isolated retina via a lens system. The firing activities of retinal GCs during response to the stimuli were simultaneously recorded by MEA using the commercial software MC_Rack (Multi Channel Systems MCS GmbH, Germany) with a sampling rate of 20 kHz and stored for off-line analyses. Spikes from individual neurons were sorted based on the principal component analysis[10] as well as the spike-sorting unit in MC_Rack. For each neuron, let t_n denote the firing time of the nth spike, then the inter-spike interval (ISI) series is obtained by

$$ISI(n) = t_{n+1} - t_n. \tag{1}$$

The first difference of the ISI (DISI) series

$$DISI(n) = ISI(n+1) - ISI(n) \tag{2}$$

is also obtained. For an unknown system, let $x_i (i = 1, \cdots, n)$ be the measured time series of a state variable. The time delay embedding method is employed to reconstruct the phase space $\boldsymbol{X}$ for an embedding dimension of d and a lag time of τ as follows:

$$\boldsymbol{X}_m = (x_m, x_{m+\tau}, \cdots, x_{m+\tau(d-1)}), \tag{3}$$

where $m = n - \tau(d-1)$ is the number of points on the reconstructed space. Based on the concept of the phase space reconstruction, different chaotic time series methods have been proposed.

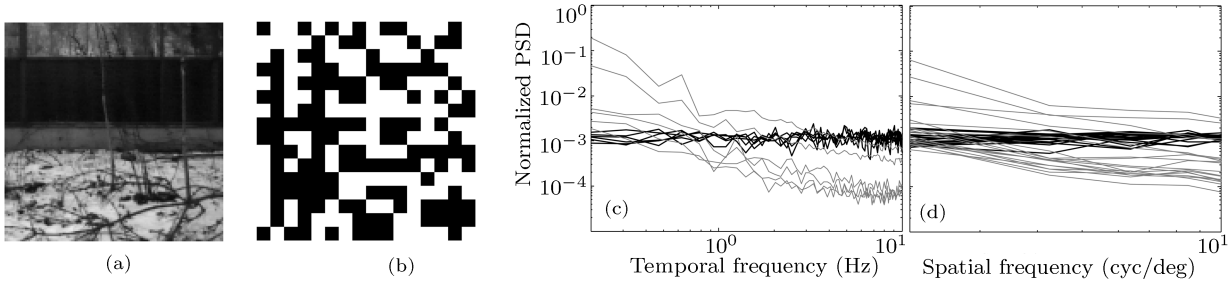

Fig. 1. Sample frames and normalized power spectral densities (PSDs) of the two kinds of stimuli. (a) A sample frame of the natural movie (displayed in a 128×128 grid). (b) A sample frame of the checker-board (displayed in a 16×16 grid). (c) The temporal frequency normalized PSDs of the natural movie (gray thin curves) and checker-board (black thick curves). The temporal frequency normalized PSDs are shown in a range of spatial frequencies and each curve denotes a certain spatial frequency. (d) The spatial frequency normalized PSDs of the natural movie (gray thin curves) and checker-board (black thick curves). The spatial frequency normalized PSDs are shown in a range of temporal frequencies and each curve denotes a certain temporal frequency.

Grassberger and Procaccia proposed a simple method to determine the attractor's correlation dimension.[2] In a d-dimensional embedding, the correlation integral is defined as the normalized number of pair of vectors that have Euclidean distance less than r:

$$C(r) = \frac{1}{m^2} \sum_{i \neq j}^{m} \Theta(r - \|\boldsymbol{X}_i - \boldsymbol{X}_j\|), \tag{4}$$

where $C(r)$ is the correlation integral, $\| \ \|$ represents the Euclidean distance and Θ is the Heaviside function. For small values of r, the correlation integral function $C(r)$ behaves according to a power law:

$$C(r) \propto r^v. \tag{5}$$

The correlation dimension of the attractor can be estimated from the curves of $\log C(r) \sim \log r$ and the onset of the plateau known as the scaling region in local slope curves indicates the occurrence of determinism. Although the correlation dimension method has the advantage of simplicity, limitations still exist such as the need of large amount of data. Furthermore, since the correlation dimension method only concerned with the static values of the data, the influence of noise is almost unavoidable.

Sugihara and May proposed a nonlinear forecasting method to measure the predictability of a dynamical system.[3] Sauer extended this method and defined a normalized prediction error (NPE) to evaluate the accuracy of the prediction.[4] For one index point $\boldsymbol{X}_i$ in the embedding space $\boldsymbol{X}$,$\{\boldsymbol{X}_j\}_{j=1,\cdots,k}$ are its k nearest neighbours. With a translation horizon of $H (H \geq 0)$ time steps ahead, the prediction is the average translation given by

$$\langle \boldsymbol{v} \rangle = \frac{1}{k} \sum_{j=1}^{k} \boldsymbol{X}_{j+H}. \tag{6}$$

The difference between the actual and average translation is the prediction error:

$$\varepsilon_{\text{pred}} = |\boldsymbol{X}_{i+H} - \langle \boldsymbol{v} \rangle|. \tag{7}$$

The prediction error for the mean of the time series is

$$\varepsilon_{\text{mean}} = |\boldsymbol{X}_{i+H} - \langle x \rangle|, \tag{8}$$

where $\langle x \rangle$ indicates the average value of $x_i (i = 1, \cdots, n)$. Then the normalized prediction error (NPE) for a translation horizon of H is

$$NPE(H) = \frac{\text{rms}(\varepsilon_{\text{pred}})}{\text{rms}(\varepsilon_{\text{mean}})}, \tag{9}$$

where rms indicates root mean square. If the value of $NPE(H)$ is less than 1.0 distinctly when $H \geq H_0$, it indicates that there exists predictability in the time series and H_0 reflects the degree of the determinism. The larger the value of H_0 is, the higher the degree of the determinism is.

The embedding dimension and the number of nearest neighbours, d and k, are optimized according to the method described by Schiff and co-workers.[11] Firstly, search for the minimum value of NPE as a function of $d = 1, 2, \cdots, d_{\max}$ with $k = 1$. The optimal embedding dimension d_{opt} is set to the value of d that corresponds to the minimum NPE. Secondly, search for the minimum value of NPE as a function of $k = 1, 2, \cdots, k_{\max}$ with $d = d_{\text{opt}}$. Similarly, the optimal number of nearest neighbours, k_{opt}, is set to the value of k that corresponds to the minimum NPE.

Compared with the correlations dimension method, the nonlinear forecasting method analyses the time series dynamically and works for a relatively short time series. Thus it has become one of the most important tools to analyse the experimental data.

In order to assess the predictability of the original data, the surrogate data are applied to produce statistical controls.[12] The surrogate data refer to datasets that preserve certain linear statistical properties of the original data, such as mean, variance, power spectrum, etc. Namely, the nonlinear deterministic component of the original data is excluded in its surrogate data. In the present study, the surrogate data are generated using the random shuffled (RS) method with the null hypothesis that the original data are independent and identically distributed. The RS surrogate data are generated as follows. Firstly, a Gaussian-distributed time series $G(t)$ with the same length to the original data $S(t)$ is generated. Secondly, the RS surrogate data $RS(t)$ are obtained by rearranging $S(t)$ following the magnitude order of $G(t)$.

The firing activities of totally 29 retinal GCs were simultaneously recorded. We take one retinal GC as an example to show the analytical results of the correlation dimension method and the nonlinear forecasting method. According to Eq. (1), the ISI series corresponding to the retinal GC during response to natural movie was obtained. Then the DISI series was obtained according to Eq. (2). A segment (length=1024) of the ISI series and a segment (length=1024) (obtained from the same segment of the original recording data) of the DISI series are analysed using the correlation dimension method and the nonlinear forecasting method. The ISI and DISI series corresponding to the retinal GC during response to checker-board are obtained and analysed similarly.

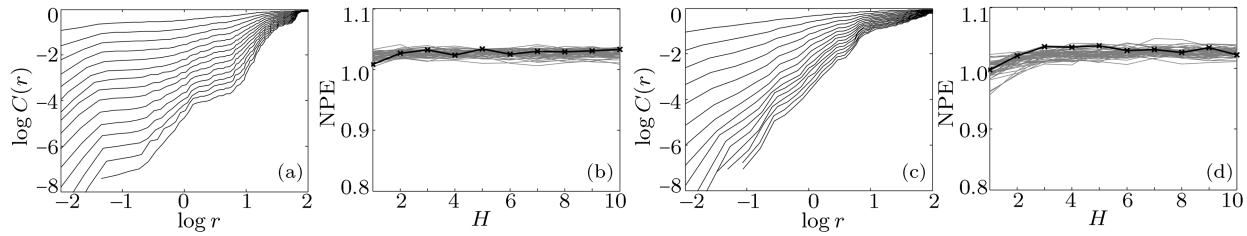

Fig. 2. Analytical results of the ISI series. (a) The $\log C(r) \sim \log r$ curves of the ISI series derived from the retinal GCs during response to natural movie. The 15 curves from top to bottom are with different values of the embedding dimension d varying from 2 to 30 with steps of 2. (b) The NPEs of the ISI series derived from the retinal GCs during response to natural movie (black thick curve, marked by crosses) and 49 sets of RS surrogate data (gray thin curves) versus H, where H is the number of steps ahead of the index point. (c) The $\log C(r) \sim \log r$ curves of the ISI series derived from the retinal GCs during response to checker-board. (d) The NPEs of the ISI series derived from the retinal GCs during response to checker-board (black thick curve, marked by crosses) and 49 sets of RS surrogate data (gray thin curves) versus H.

Figure 2 illustrates the analytical results of the correlation dimension method and the nonlinear forecasting method for the ISI series derived from the retinal GC during response to natural movie (Figs. 2(a) and 2(b)) and checker-board (Figs. 2(c) and 2(d)). As shown in Figs. 2(a) and 2(c), there is no stable linear region in the $\log C(r) \sim \log r$ curves, which implies that the correlation dimension method fails to show any evidences for the existence of underlying determinism in the ISI series. As shown in Figs. 2(b) and 2(d), the NPEs of the ISI series approximately equal to 1.0 even when $H = 1$ and cannot be separated from that of the RS surrogate data, which indicates that there is no predictability in the ISI series beyond the baseline prediction of the series mean. In other words, no determinism is detected in the ISI series.

The ISI series derived from the other 28 retinal GCs are analysed in the same way and similar analytical results are obtained.

Figure 3 illustrates the analytical results of the DISI series derived from the retinal GC during response to natural movie (Figs. 3(a) and 3(b)) and checker-board (Figs. 3(c) and 3(d)). As shown in Figs. 3(a) and 3(c), there is still no stable linear region in the $\log C(r) \sim \log r$ curves, which implies that the correlation dimension method fails again to show any evidences for determinism. As shown in Figs. 3(b) and 3(d), only the one-step-ahead NPE($H = 1$) of the DISI series is less than 1.0 and can be apparently separated from that of the RS surrogate data, which indicates that there exists distinct predictability in the DISI series. Furthermore, the one-step-ahead NPE is close to 1.0, which indicates that the degree of predictability is weak. The DISI series derived from the other 28 retinal GCs are analysed in the same way and similar analytical results are obtained.

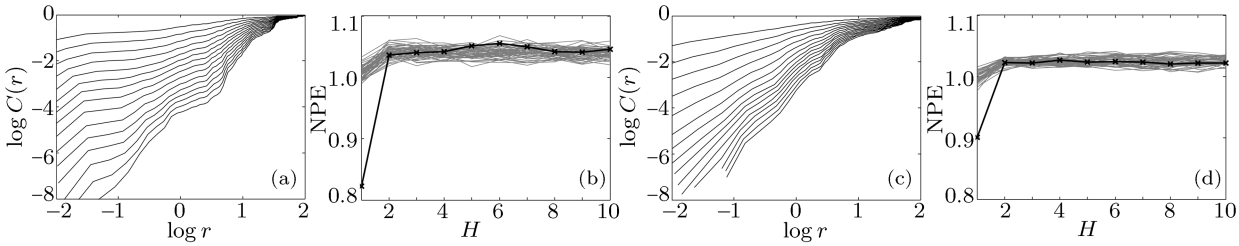

Fig. 3. Analytical results of the DISI series. (a) The $\log C(r) \sim \log r$ curves of the DISI series derived from the retinal GCs during response to natural movie. (b) The NPEs of the DISI series derived from the retinal GCs during response to natural movie (black thick curve, marked by crosses) and 49 sets of RS surrogate data (gray thin curves) versus H. (c) The $\log C(r) \sim \log r$ curves of the DISI series derived from the retinal GCs during response to checker-board. (d) The NPEs of the DISI series derived from the retinal GCs during response to checker-board (black thick curve, marked by crosses) and 49 sets of RS surrogate data (gray thin curves) versus H.

In conclusions, firstly, the first difference operation of the ISI series makes it comparatively easier for determinism detection in the firing activities of retinal GCs. There is no doubt that noise derived from measurement and spike sorting procedure plays a negative role during the course of determinism detection, which may result in the failure when the correlation dimension method and the nonlinear forecasting method are applied. Therefore, it seems that the first difference operation has the ability to reduce noise. However, why does the first difference operation has this ability? Answer to this question needs more theoretical analysis and experiments in the future. Secondly, the nonlinear forecasting method is more efficient and reliable than the correlation dimension method for determinism detection. The advantage of the nonlinear forecasting method results partly from the effect of noise reduction through the process of summation and average operation of the nearest neighbour points.

References

[1] Touryan J and Dan Y 2001 *Curr. Opin. Neurobiol.* **11** 443
[2] Grassberger P and Procaccia I 1983 *Phys. Rev. Lett.* **50** 346
[3] Sugihara G and May R M 1990 *Nature* **344** 734
[4] Sauer T 1994 *Phys. Rev. Lett.* **72** 3811
[5] Jeong J, Gore J C and Peterson B S 2002 *Biol. Cybern.* **86** 335
[6] Xu J X, Gong Y F, Ren W, Hu S J and Wang F Z 1997 *Phys.* D **100** 212
[7] Gong Y F, Xu J X, Ren W, Hu S J and Wang F Z 1998 *Biol. Cybern.* **78** 159
[8] Chen A H, Zhou Y, Gong H Q and Liang P J 2004 *Brain Res.* **1017** 13
[9] Chen A H, Zhou Y, Gong H Q and Liang P J 2005 *Neuroreport* **16** 371
[10] Zhang P M, Wu J Y, Zhou Y, Liang P J and Yuan J Q 2004 *J. Neurosci. Meth.* **135** 55
[11] Schiff S J, So P and Chang T 1996 *Phys. Rev.* E **54** 6708
[12] Theiler J, Eubank S, Longtin A, Galdrikian B and Farmer J D 1992 *Phys.* D **58** 77